energies

MDPI

Article

Thermodynamic and Economic Feasibility of Energy Recovery from Pressure Reduction Stations in Natural Gas Distribution Networks

Piero Danieli *, Gianluca Carraro and Andrea Lazzaretto

Department of Industrial Engineering, University of Padova, 35122 Padova, PD, Italy; gianluca.carraro.4@studenti.unipd.it (G.C.); andrea.lazzaretto@unipd.it (A.L.)

* Correspondence: piero.danieli@unipd.it

Received: 24 July 2020; Accepted: 27 August 2020; Published: 28 August 2020

Abstract: A big amount of the pressure energy content in the natural gas distribution networks is wasted in throttling valves of pressure reduction stations (PRSs). Just a few energy recovery systems are currently installed in PRSs and are mostly composed of radial turboexpanders coupled with cogeneration internal combustion engines or gas-fired heaters providing the necessary preheating. This paper clarifies the reason for the scarce diffusion of energy recovery systems in PRSs and provides guidelines about the most feasible energy recovery technologies. Nine thousand PRSs are monitored and allocated into 12 classes, featuring different expansion ratios and available power. The focus is on PRSs with 1-to-20 expansion ratio and 1-to-500 kW available power. Three kinds of expanders are proposed in combination with different preheating systems based on boilers, heat pumps, or cogeneration engines. The goal is to identify, for each class, the most feasible combination by looking at the minimum payback period and maximum net present value. Results show that small size volumetric expanders with low expansion ratios and coupled with gas-fired heaters have the highest potential for large-scale deployment of energy recovery from PRSs. Moreover, the total recoverable energy using the feasible recovery systems is approximately 15% of the available energy.

Keywords: energy recovery; natural gas distribution network; natural gas expander; natural gas engineering; economic analysis

1. Introduction

The natural gas network is designed to achieve an acceptable compromise between cost of infrastructure and cost of the energy spent to pressurize the gas. To reduce the volume of pipelines and make the transportation efficient, the natural gas is compressed before the injection in the distribution network [1]. However, just a small fraction of the pressure energy of the natural gas is effectively utilized to keep it in motion while the rest is usually wasted in pressure reduction stations (PRSs). These stations subdivide the distribution network into subsystems working at decreasing pressure levels as the gas gets closer to the final users. For instance, the maximum distribution pressure for domestic units is 0.04 barg, whereas it ranges from 8 barg to 0.04 barg for industrial users and energy conversion plants. To guarantee the availability of natural gas at the various extraction points and make the interaction possible between subsystems operating at different pressure levels, the natural gas network is equipped with various pressure reduction stations (PRSs). In these stations, the pressure drop of the natural gas is obtained by means of simple and reliable throttling valves, which perform an isenthalpic process without any extraction of work. Alternatively, energy recovery technologies can be used to exploit the energy associated with the pressure drop for power generation. The scientific literature agrees that one of the most feasible energy recovery technologies for PRSs is the radial turboexpander-generator.

However, this machine is quite expensive (also because it generally requires a gearbox) and, therefore, becomes more convenient as the size increases. Real installations of radial-turboexpander generators have worked profitably for years in several countries (e.g., in the US [2], UK [3], and Italy [4,5]). However, the number of installed machines is still relatively modest. Recently, a few authors proposed volumetric expanders instead of the traditional radial ones because of the lower cost and higher robustness. These features start to become increasingly important as the size of the energy system decreases and, for very small sizes, it may become necessary to pay off the investment costs in reasonably short periods. Diao et al. [6] developed a prototype of a screw expander working with natural gas between 8 barg and 2 barg, finding an isentropic efficiency of about 70%. Howard et al. [7] studied an energy recovery solution including a small size radial turboexpander coupled to fuel cells for preheating and working between 6 barg and 2 barg. They found an averaged isentropic efficiency of the expander of about 68%. Yao et al. [8] carried out a study on the performance of a twin-screw expander as power generation unit working with natural gas between average pressures of 8 barg and 2 barg. They found that the expander could reach isentropic efficiencies of about 70% at design conditions, which decrease to 35% at off-design conditions. Yaxuan et al. [9] considered the energy recovery from a natural gas network with a single-screw expander coupled with a heat pump to provide the energy needed for preheating. The expander works both as power generation unit and pressure regulation device between 6 barg and 1 barg, and shows an isentropic efficiency ranging between 90% and 40%. Tian et al. [10] developed a mathematical model to predict the performance of a single-screw expander employed in steam pressure pipelines to recover energy from the pressure drop (7 barg – 1 barg) during intermittent operating conditions. They found that the maximum isentropic efficiency fluctuates between 73 and 83%. Barbarelli et al. [11] developed a prototype of an innovative volumetric expander to recover energy from natural gas from a pressure drop of 3.5 – 1 barg with a maximum achievable isentropic efficiency of about 40%. Kolansky et al. [12] conducted a thermodynamic analysis on rolling piston expanders adopted to recover the pressure energy of natural gas. They found that the expander was able to achieve an isentropic efficiency of about 60% working with expansion ratio of 2. Some works deal with the optimization of reciprocating piston expanders using exergy analysis in energy recovery applications in natural pressure reduction stations [13,14]. They all suggest that this expansion system could have a high potential in the proposed application. As imposed by the Italian legislation, most of the expander installations require the preheating of natural gas before the expansion process. This avoids the undesired condensation of gas hydrates that could damage pipelines and other components of the network but, in contrast, it reduces the advantages of gas expanders in terms of energy efficiency. Thermal oil or water heaters are employed as gas preheaters because of the relatively low cost. However, numerous works in the literature propose the utilization of different strategies to manage the preheating and increase the total efficiency of the system, such as:

(1) Using a solar thermal storage [15] or low-temperature thermal sources deriving from industrial processes and renewables [16,17].
(2) Coupling (e.g., [18]) heat pumps with the turboexpander electric generator to invest part of the electricity generated by recovery for preheating.
(3) Utilizing the cold thermal energy available at the end of the expansion process for industrial or domestic users [19] or as a cold source for power plants [20].
(4) Using cogenerative (CHP) internal combustion engines (ICEs) to supply the thermal power output for gas preheating and produce an additional electric power output [21].

In any case, the electricity generated by the expander-generator can be sent to the grid, used for preheating, or stored in the gas network as hydrogen [19,22,23].

It is evident that this field represents an active research area in which a wide range of possible energy recovery solutions can be applied to PRSs. However, real applications are still very limited despite the stricter policies for energy saving adopted recently in several countries. In this context,

some questions arise: Why is the energy recovery from PRSs in natural gas distribution network rarely proposed? Is it a matter of costs or efficiency? Are there one or more energy recovery solutions that could be feasible for a diffuse application to a large number of PRSs? How much energy can be recovered with acceptable costs and efficiency?

The goal of this paper is to answer these questions by identifying the most economically feasible energy recovery solutions that could be employed in various "classes" of pressure reduction stations featuring different expansion ratios and annual-averaged available power. The energy recovery solutions considered in the economic evaluations were selected from among 12 commercially available systems including an expander-generator coupled to a natural gas preheating system. Available data of a large sample (9000 PRSs) of real PRSs in the Italian gas distribution network were utilized to perform the analysis and eventually to calculate the amount of energy that could be recovered utilizing the energy recovery solutions indicated by the results of the economic evaluation. The wide sample of PRSs, and the various expansion ratios and flow rates of these PRSs, made the results general and applicable also to other gas distribution networks.

2. Description of the Italian Natural Gas Distribution Network

Natural gas distribution networks are composed of three main components: Pipelines, compression stations, and pressure reduction stations (PRS). The Italian gas network features about 32,500 km of pipelines at various pressure levels, 11 recompression stations with a total installed power of about 877 MW and about 9000 monitored pressure reduction stations. The entire network is divided into two main parts:

(1) The "national pipeline network", including the systems involved in the transportation of natural gas from the injection points to the regional interconnections and storage sites, and
(2) The "regional pipelines network", including the systems required for the local transportation of natural gas and the supply of industrial/urban users and power plants.

Figure 1 shows the geographical location of the national (red) and regional (blue) pipeline networks and of the injection points from neighboring and oversea countries.

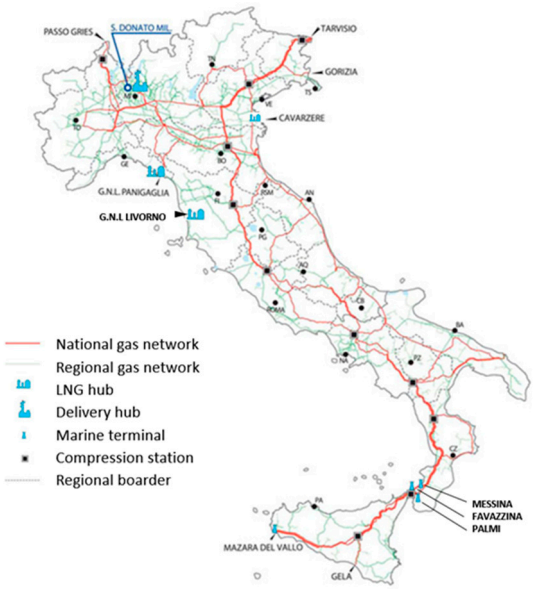

Figure 1. Italian national (red) and regional (blue) pipeline gas network. Injection points from foreign suppliers [24].

The connection with Sicily Island is guaranteed by four Marine Terminals connecting the submarine pipelines to the onshore ones in Mazara del Vallo (Trapani), Messina, Favazzina (Reggio Calabria), and Palmi (Reggio Calabria).

National reserves cover only a small fraction of the natural gas consumption in Italy, the rest being supplied through five injection points (1–5 in the following) connected to international pipelines and three injection points (6–8 in the following) connected to liquefied natural gas (LNG) hubs:

(1) Mazara del Vallo (Sicily), connected to the Algerian gas supply network by means of submarine pipelines;
(2) Gela (Sicily), connected to the Libyan gas supply network by means of the submarine pipeline called "Greenstream";
(3) Tarvisio (northeast), connected to the Austrian gas network by the Trans Austria Gas (TAG) pipeline;
(4) Gorizia (northeast), connected to the Slovenian gas network;
(5) Gries Pass (north), connected to the Swiss gas network by the Transitgas pipeline;
(6) Italia di Panigaglia, (northwest coast), connected to LNG hub;
(7) Cavarzere (northeast coast), connected to LNG hub; and
(8) Livorno (northwest coast), connected to LNG hub.

Natural gas storage sites are extremely important for the Italian market of natural gas because they highly improve the flexibility of the network and give a "safety margin" in a market strongly dependent upon imports. The total storage capacity is about 16 billion m^3 and is realized in exhausted underground deposits. Both the storage capacity and the LNG injection points are planned to be increased in the next few years.

3. Methods

The methodology applied in this paper can be summarized into the following steps:

(1) Selection of the classes of pressure reduction stations and where to perform the economic investigations;
(2) Selection of the energy recovery systems;
(3) Sizing of the energy recovery systems and calculation of the produced energy;
(4) Calculation of payback period (PBP) and net present value (NPV); and
(5) Calculation of the energy recovery efficiency.

Each step is described in the following.

3.1. Selection of PRS Classes

Detailed monitored data are available for the majority of the PRSs in the national pipeline network, whereas just a little information is available for those installed in the regional pipeline network (i.e., delivering gas to the domestic users). Gas distributors do not monitor the operation of these stations because of their secondary role in the distribution network. The annual-averaged flow rate of natural gas and inlet and outlet pressure data are available for a sample of about 9000 PRSs. Figure 2 shows the cumulative percentage distribution of the number of PRSs against (i) the annual-averaged available power (Figure 2a) and (ii) the pressure drops (Figure 2b), calculated with Equation (11).

Figure 2 shows that about 99% of the PRSs of the sample provides an annual-averaged available power between 0 and 500 kW and performs a pressure drop with an expansion ratio between 1 and 20. It is worth noting that almost 75% of PRSs show an available power lower than 10 kW. To simplify the calculations, 12 PRSs classes were identified, and for each of them a reference station was selected as representative for the analysis in the following sections. In accordance with the data in Figure 2, the total power range was subdivided in four intervals: (i) 1–10 kW, (ii) 10–50 kW, (iii) 50–200 kW, and (iv) 200–500 kW. A minimum value of 1 kW was set since there was no information about performance and costs of commercially available systems for these sizes. Similarly, the following three intervals of

pressure ratios were chosen: (i) 1–3, (ii) 3–8, and (iii) 8–20. As a result, 12 PRS classes (Figure 3) were obtained. Note that the selection of the classes had the intention to organize the results and to simplify the analysis.

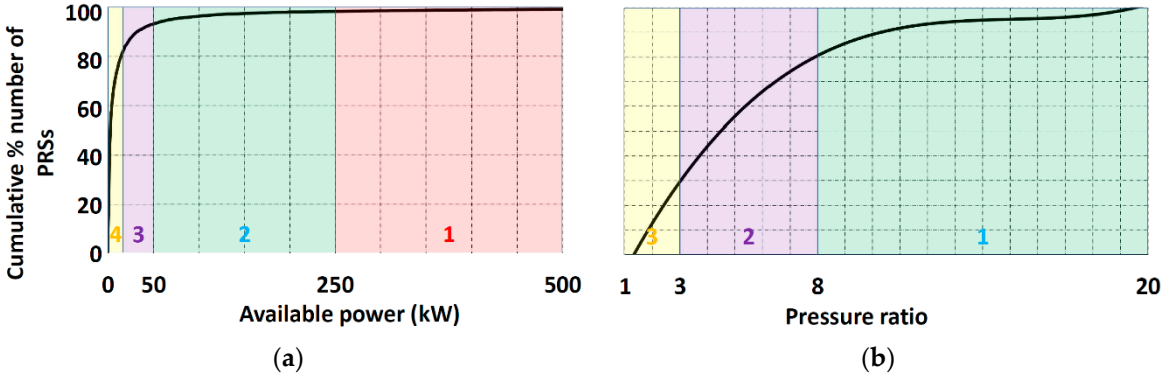

Figure 2. Cumulative percentage distribution of the number of pressure reduction stations (PRSs) (included in the available sample) against (**a**) annual-averaged available mechanical power and (**b**) pressure ratio of the processed natural gas.

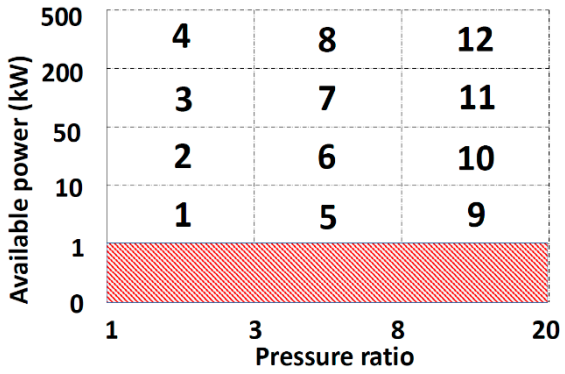

Figure 3. Ranges of available power and pressure ratios correspondent to the 12 PRS classes selected for economic and thermodynamic analysis.

3.2. Selection of the Energy Recovery Systems

Almost the entirety of the works in the literature agree that the production of electricity by expander-generators is the most appropriate way to convert the mechanical energy available from the pressure drops in the PRSs. Despite this, the features of the PRSs that make the use of turboexpanders or volumetric expanders more profitable are often still not clear. It is, therefore, important to analyze the operating characteristics and costs of each kind of expander in relation to those of the PRSs. Moreover, a key point to optimize the design and operation of the energy recovery system as a whole is the proper choice of the thermal source required to avoid an excessive cooling of the gas, which could damage valves and pipelines because of hydrates' icing. Some promising solutions such as the (1) and (3) ones listed in the Introduction are "location dependent" because they depend on the local features of the thermal sources and/or demands. Thus, they are inadequate for a large-scale diffusion. As a result, options (2) and (4) and the use of standard heaters were selected here as suitable technologies to manage the required gas preheating upstream of the expander generators. Figure 4 presents all 12 combinations among expander-generators and preheating systems considered in this work. In particular, single/double-stage radial turboexpanders and scroll expanders were selected as power conversion systems, while geothermal heat pumps, air heat pumps, gas-fired heaters, and CHP internal combustion engines were chosen as potential preheating systems. Accordingly, 12 possible combinations could be generated.

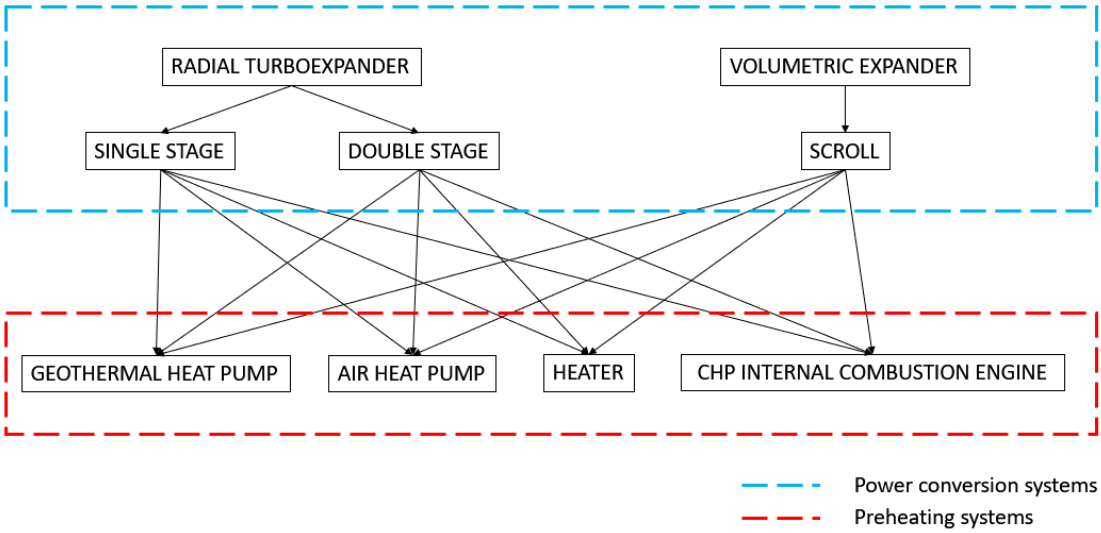

Figure 4. All possible combinations (12) among the expansion technologies and natural gas preheating systems considered in the analysis.

3.3. Sizing, Energy Consumption, and Electric Producibility of the Energy Recovery Systems

The following subsections describe the methods used to size the energy recovery systems and to predict their annual electric production and energy consumption for gas preheating.

3.3.1. Expanders

The size of the expander, identified here by the mass flow rate ($\dot{m}_{DP}$) at design point, should be selected for each PRS in accordance with the annual trend of the natural gas mass flow rate, which is strongly affected by the seasonality of consumptions. Figure 5 shows the dimensionless curve of the natural gas mass flow rate derived from measured data of a real PRS installed in Padova (classified in class 2 of Figure 3). To simplify the calculations, this curve was substituted by a five-steps curve, keeping the total area below the curve unchanged, and was then used to reproduce the mass flow rate curves in all PRSs. This was done multiplying, for each PRS, the dimensionless mass flow rate of each step in Figure 5 by the known value of the annual-average mass flow rate through the PRS. Using the same trend for all the PRS classes reduces the accuracy of the calculation but strongly simplifies it. The loss in accuracy obviously depends on the kind of PRS that is considered. Certainly, it will not be high for the main cities in the northern part of Italy, where the trend of natural gas consumption (Figure 5) is similar to that of Padova. In any case, this trend shows a quite high difference between maximum and minimum consumption, which imposes a challenging task for the choice of the expander size. Similar trends are expected also for the mainland areas of Europe. The expected trends at lower latitudes are flatter, making the choice of the expander size easier.

The expander was sized for six different values of design point mass flow rates selected in between the maximum ($\dot{m}_{step=1,PRS}$) and minimum values ($\dot{m}_{step=3,PRS}$) by dividing equally the operating field ($\dot{m}_{step=1,PRS} - \dot{m}_{step=3,PRS}$) in Figure 5. For each of the six possible sizes, the annual producible electric energy was calculated, using Equation (1), while the design point electric power output was calculated by using Equation (2).

$$E_{el,exp} = \sum_{step=1}^{5} \dot{m}_{step} \cdot \Delta h_{is,step} \cdot \eta_{is,step} \cdot \Delta t_{step} \cdot \eta_{el} \quad (1)$$

$$P_{el,DP} = \dot{m}_{DP} \cdot \Delta h_{is,DP} \cdot \eta_{is,DP} \cdot \eta_{el} \quad (2)$$

where $E_{el,exp}$ (kWh/y) is the annual electricity producible by the expander, $\dot{m}$ (kg/s) is the expander mass flow rate, Δh_{is} (kJ/kg) is the isentropic enthalpy drop, η_{is} (-) is the isentropic efficiency, and Δt_{step}

[h] is the time interval of each step. The values of the performance parameters at design point were set in accordance with those normally adopted in the design of the considered types of expander (Table 1). For single-stage, radial-turboexpanders, the blade tip speed (U) was limited to a maximum value of 400 m/s. This constraint on the blade tip speed was achieved by choosing properly the enthalpy drop through the expander ($\Delta h_{is} = \frac{C_0^2}{2}$, where C_0 is the isentropic spouting velocity), with the tip-speed ratio ($\frac{U}{C_0} = 0.7$) at design point determined by the search of the optimal fluidynamic behavior [25]. Thus, a pressure regulation system (with valves) is generally necessary before the expansion to adjust the available enthalpy drop to the optimum one chosen for the expander. This adjustment reduces the pressure drop without extraction of mechanical work because of the isenthalpic process in the valves. The loss in potential mechanical work is higher with single-stage machines, and can be reduced, increasing the number of stages (the total Δh_{is} was allocated in multiple stages and, therefore, the tip speed of each stage could satisfy the design point constraints without adjustments of the pressure drop). Double-stage, radial-turboexpanders were evaluated here (in addition to the single-stage ones) only for PRSs having a too high expansion ratio for a single-stage optimal machine, because they would entail higher costs without increasing the power production. In these cases, we kept the same ideal enthalpy drop in each stage by fixing the stage exit temperature and, so, evaluating also the intermediate pressure. This criterion established, in turn, the maximum temperature of preheating in each stage. Figure 7 shows the thermodynamic processes in a dual-stage turbine, expanding natural gas between 50 and 10 bar. As mentioned above, the ideal enthalpy drop and the outlet temperature were set equal for the two stages. An iterative procedure allowed us to calculate the intermediate pressure between the two stages that satisfied the enthalpy drop and outlet temperature constraints. Scroll expanders were considered always as single-stage machines.

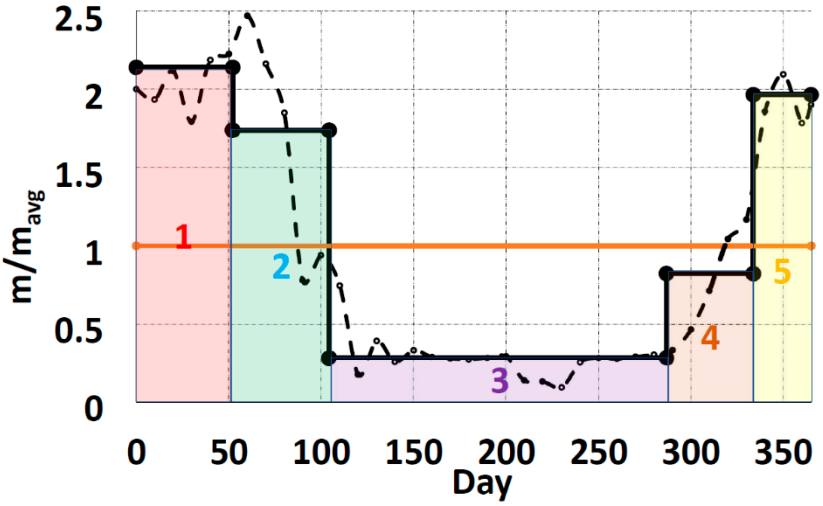

Figure 5. Dimensionless step (linked dots) and original (dashed line) function of the natural gas mass flow rate flowing through a reference PRS.

Table 1. Design parameters of radial and scroll expanders.

Design Parameters	Radial Turboexpander	Scroll Expander
Design point isentropic enthalpy difference ($\Delta h_{is,DP}$)	$f(p_{in,PRS}, p_{out,PRS}, T_{in,PRS}, U)$	$f(p_{in,PRS}, p_{out,PRS}, T_{in,PRS})$
Tip-speed-ratio ($U/\sqrt{2 \cdot \Delta h_{is,DP}}$)	0.7	-
Isentropic efficiency ($\eta_{is,DP}$)	0.85	See Figure 6
Electric motor efficiency (η_{el})	0.9	0.9
Rotational speed (rpm)	Variable	Variable

Inlet temperature (T_{in}) is imposed by the preheating.

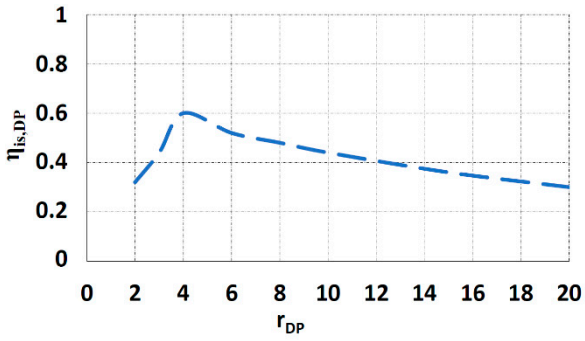

Figure 6. Isentropic efficiency corresponding to the selected design point expansion ratio for scroll expanders.

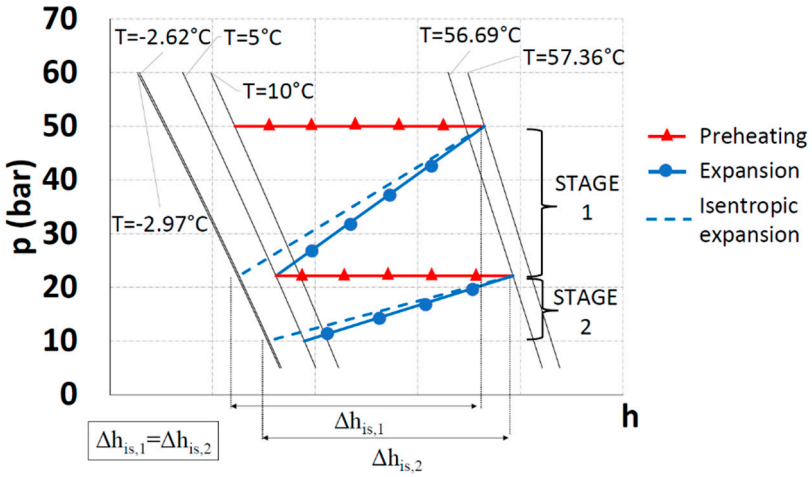

Figure 7. Thermodynamic processes (pressure-enthalpy diagram) in a dual-stage turbine working between 50 and 10 bar, considering equal isentropic enthalpy drops of the two stages and 5 °C as minimum natural gas temperature after expansion process.

The isentropic efficiency of scroll expanders strongly depends on the volumetric losses, which are directly correlated to the expansion ratio (the design features of the scroll expanders do not allow a perfect sealing, which involves increasing volumetric losses, increasing the pressure ratio). Accordingly, the design point isentropic efficiency of scroll expanders was considered as a function of the design point expansion ratio (r_{DP}), as described in Figure 6. This trend was derived by the experimental data of a scroll expander, which uses air as working fluid [26]. For a first approximation, the same performance was considered for air or natural gas.

The annual producible electricity of the expanders was calculated, taking into account the off-design operation and considering the following assumptions:

- When the design value of the expander mass flow rate at design point ($\dot{m}_{DP}$) is lower than the mass flow rate in a step of Figure 5 (i.e., $\dot{m}_{DP} < \dot{m}_{step,PRS}$), the expander operates at design point conditions and, therefore, a part of the mass flowrate is bypassed. As a result, the operating parameters in Equation (1) were set as follows;

$$\dot{m}_{step} = \dot{m}_{DP};\ \Delta h_{is,step} = \Delta h_{is,DP};\ \eta_{is,step} = \eta_{is,DP} \tag{3}$$

- When the mass flow rate is lower than the design one ($\dot{m}_{step,PRS} < \dot{m}_{DP}$), the expander works at partial load, and the operating parameters required in Equation (1) were calculated as follows:

$$\dot{m}_{step} = \dot{m}_{step,PRS};\ \Delta h_{is,step} = \Delta h_{is,DP}; \eta_{is,step} = f\left(\dot{m}_{step,PRS}\right) \tag{4}$$

As shown in Equation (4), the mass flow rate of the expander was set equal to that of the PRS' in the considered step, while the enthalpy drop was kept at the design point value by varying the rotational speed. The isentropic efficiency of the radial turboexpander at partial load was evaluated considering the dimensionless trend in Figure 8a. Given the mass flow rate at partial load ($\dot{m}_{step}$), the corresponding isentropic efficiency can be evaluated. This trend was obtained by resizing the experimental curve provided by [27], using the design point mass flow rate and isentropic efficiency. The radial turboexpander, considered as reference [27], had a variable geometry control system and variable rotational speed and used natural gas as working fluid. To a first approximation, the radial turboexpanders designed in the analysis achieved the same design point efficiency regardless of their size and performed equally at part-load operations (in relation to their design point mass flow rate). This is consistent with the relatively modest variation of the expander size and with the detailed level of the current analysis. Similarly, the part-load isentropic efficiency of scroll expanders was calculated considering the dimensionless efficiency curve in Figure 8b, derived from experimental data provided in [26].

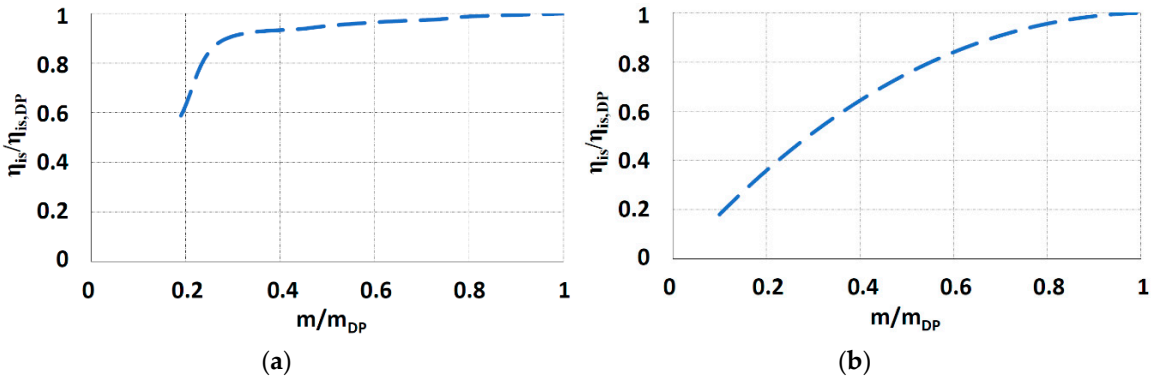

Figure 8. Trend of the isentropic efficiency resized using the design point value against the part-load mass flow rate of (**a**) radial turboexpanders and (**b**) scroll expanders.

3.3.2. Preheating Systems

The thermal power needed for preheating is calculated using the following equations:

$$Q_{th} = \frac{\dot{m}_{gas} \cdot \Delta h_{ph}}{\eta_{HE}} \tag{5}$$

$$\Delta h_{ph} = f\left(p,\ T_{out,ph}\right) - f\left(p,\ T_{in,ph}\right) \tag{6}$$

$$T_{out,ph} = f(\Delta h_{is}, \eta_{is}) \tag{7}$$

where Q_{th} (kW) is the thermal power needed for the preheating process, Δh_{ph} (kJ/kg) is the enthalpy increase resulting from preheating, $T_{in,ph}$ is the gas inlet temperature (depending on the season), p (bar) is the gas pressure, and η_{HE} is the efficiency of heat exchangers (0.90). $T_{out,ph}$ is the gas temperature after preheating, which depends on the expansion process. This temperature is subject to the constraint that natural gas should not exit the PRS (after the expansion) at a lower temperature than 5 °C. This constraint was imposed by the Italian legislation to avoid the condensation of hydrates in the gas network. Equations (5)–(7) show that the preheating thermal power is a function of the expander mass flow rate and enthalpy drop but also of the natural gas temperature (that varies during the year). For each size of the expander, the size of the preheating system was defined by the thermal power required before the expansion during the most demanding operation, i.e., during the winter season (step 1 or 5). Table 2 lists the temperature of natural gas at the inlet of PRSs and the ambient temperature considered in each time step.

Table 2. Natural gas and ambient temperature in the five time steps.

Steps	Gas Inlet Temperature (°C)	Ambient Temperature (°C)
1	10	5.5
2	12	10
3	15	20.6
4	13	12.25
5	10	5.5

The energy consumption of the preheating systems was calculated using the following equations:

$$\text{Heat pumps} \qquad E_{el,HP} = \sum_{step=1}^{5} \frac{Q_{ph,step}}{COP_{step}} \cdot \Delta t_{step} = \sum_{step=1}^{5} P_{el,step} \cdot \Delta t_{step} \tag{8}$$

$$\text{CHP-ICE, Gas fired heaters} \qquad E_{fuel} = \sum_{step=1}^{5} \frac{Q_{ph,step}}{\eta_{th,\ step}} \cdot \Delta t_{step} = \sum_{step=1}^{5} Q_{fuel,step} \cdot \Delta t_{step} \tag{9}$$

The coefficient of performance (COP_{step}) of the heat pumps was affected by the temperatures of the cold and hot source (T_{evap}, T_{cond}, respectively). The temperature of the hot source (T_{cond}) was the temperature of natural gas after preheating (i.e., $T_{out,ph}$). The evaporation temperature (T_{evap}) of the geothermal heat pump was set equal to 15 °C, which is the average annual ground temperature in Italy. To a first approximation, the heat transfer area between ground and working fluid of the heat pump was considered infinite. The evaporation temperature (T_{evap}) of the air heat pump was set 5 °C lower than the ambient temperature considered in each time step (see Table 2). The COP is then evaluated using commercial data (Figure 9) supplied in [28,29] (these two papers refer to the performance of geothermal and air heat pumps, respectively).

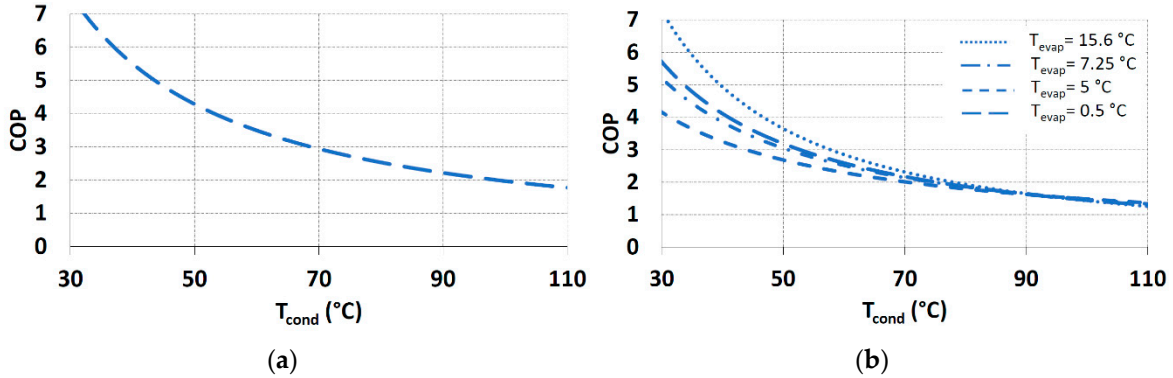

Figure 9. Coefficient of performance (COP) corresponding to (**a**) geothermal and (**b**) air heat pump against hot source temperature (T_{cond}).

The thermal efficiency of gas-fired heaters at design point was set at 0.9. At partial-load operations, the performance of the heaters was predicted using the dimensionless efficiency curve in Figure 10, derived by the experimental data of a reference heater provided by manufacturers [30].

Thermal oil and water gas-fired heaters feature the same design and off-design performance. The choice between one of the two depends on the preheating temperature: Water heaters are considered up to 90 °C, while thermal oil heaters are considered for higher temperatures. The thermal and electric efficiency of CHP-ICEs at design point was set equal to 0.47 and 0.4 [31]. ICEs are fueled with natural gas and recover thermal energy from the cooling systems and exhaust gases. Partial-load performance was obtained by resizing real data [31] using design point parameters. The resulting dimensionless efficiency curves are shown in Figure 10. The electricity production of CHP-ICEs was evaluated by multiplying the preheating energy consumption by the electric efficiency of the engines (Figure 10).

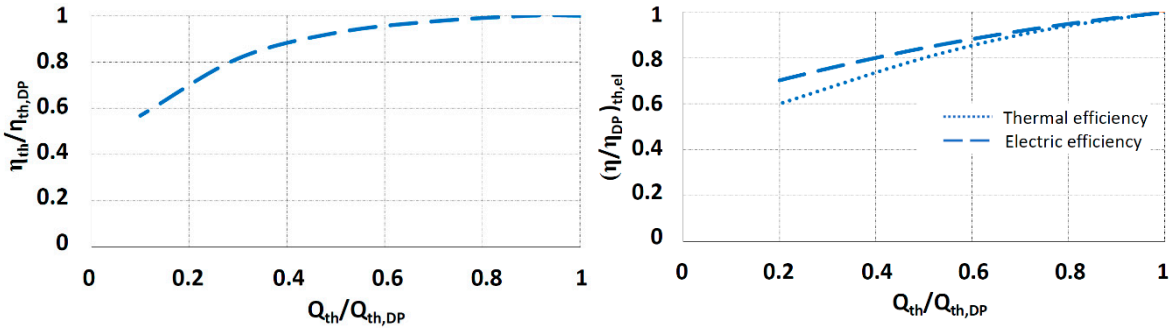

Figure 10. Trend of the thermal/electric efficiency resized using the design point values against the part-load thermal power needed by the preheating process of (**a**) gas-fired heaters and (**b**) cogenerative internal combustion engines (CHP-ICE).

3.4. Annual Available and Recoverable Energy from the PRSs

The annual energy made available by the pressure drop in a PRS is calculated using Equation (10):

$$E_{av} = \sum_{step=1}^{5} \left(\dot{m}_{step} \cdot \Delta h_{is,step} - Q_{th,step}\right) \cdot \Delta t_{step} \tag{10}$$

$$P_{av,avg} = \frac{E_{av}}{8760}. \tag{11}$$

Note that $Q_{th,step}$ (kW) is the preheating needed when the pressure energy content is dissipated with the standard throttling valves commonly installed in the stations. Accordingly, $Q_{th,step}$ is often null because the cooling deriving from the isenthalpic process allows satisfying the temperature constraint imposed by the legislation without any preheating. The energy recovery efficiency is calculated using the following equation:

$$\varepsilon = \frac{E_{exp} - E_{ph}}{E_{av,net}} = \frac{\frac{E_{el,exp} - \left(E_{el,HP}\right)}{\eta_{el,\ ref}} - \frac{E_{ph}}{\eta_{th}}}{E_{av,net}} \tag{12}$$

where E_{exp} (kWh) is the annual primary energy produced by the expander-generator, E_{ph} (kWh) is the annual primary energy consumed for preheating, $\eta_{el,\ ref}$ is the reference efficiency for the electricity production, and η_{th} is the thermal efficiency of the considered preheating system. Note that in case of heat pumps, E_{ph} must be considered null and E_{exp} is the amount of electricity spent in the heat pump for preheating.

3.5. Economic Evaluations

The goal of the economic analysis was to calculate the PBP and NPV of the energy recovery systems deriving from: the 12 proposed configurations (Figure 4), the six considered sizes (Section 3.3), and the 12 PRS classes (Figure 3). The analysis was performed for one reference station per class having available power and pressure ratio approximately equal to the average between the upper and lower limits of its class. This simplification did not involve remarkable variations of the results, considering the objective of the current analysis. Taking into account 12 classes, 12 energy recovery systems and six possible sizes, 864 cases were evaluated. The PBP and the NPV were calculated as:

$$\sum_{year=1}^{PBP} NPV_{(year)} - F_0 = F_{(year)} \cdot (1+k)^{-year} - F_0 = 0 \tag{13}$$

where $F_{(year)}$ is the cash flow in the year being considered, k (=0.015) is the discount rate, and F_0 is the investment cost. The cash flow takes into account (i) the revenues deriving from selling the electricity to the grid, (ii) the costs of operation, (iii) the cost of maintenance, and (iv) the taxes imposed by the Italian legislation to the electricity generation.

3.5.1. Cost of the Investment and Maintenance

The investment costs of the turboexpander-generators, scroll expander-generators, thermal oil heaters, and water heaters were evaluated using the module costing technique (MCT) proposed by Turton et al. [32]. The MCT evaluates the "bare module equipment cost" (CBM in Equation (14)), which is the sum of direct and indirect costs of a specific component.

$$C_{BM} = C_P^0 \cdot F_{BM} \cdot Y \tag{14}$$

$$log_{10}\left(C_P^0\right) = K_1 + K_2 \cdot log_{10}(A) + K_3 \cdot log_{10}^2(A) \tag{15}$$

$$Y = \frac{CEPCI_{2019}}{CEPCI_{2001}} = \frac{619.2}{397} = 1.56 \tag{16}$$

$C_P{}^0$ is the purchase cost of the equipment at "base conditions" (equipment composed by standard materials, working at standard pressure and temperature conditions), which does not include direct and indirect costs associated with installation material, piping, insulation, fireproofing, foundations, structural supports, instrumentation, electrical equipment, installation labor, transportations, insurance, salaries, temporary buildings, etc. The "bare module factor" (F_{BM}) in Equation (14) was given as a multiplier to keep into consideration all these additional costs for the considered equipment (Table 3). $C_P{}^0$ is calculated using Equation (15) where A is the size parameter (kW) and the coefficients K_1, K_2, and K_3 are specific for each component (Table 3). The MCT was updated using the Chemical Engineering Plant Cost Index (CEPCI) of 2019 (multiplying factor Y in Equation (16)).

Table 3. MCT cost coefficients.

Component	Size	Size Range	K_1,K_2,K_3	F_{BM}
Radial turboexpander	W (kW)	10–6000	2.2476 1.4965 −0.1618	1
Electric drives (Radial turboexpander)	W (kW)	10–6000	2.4604 1.4191 −0.1798	3.5
Scroll expander	W (kW)	10–100	3.1507 1.4965 −0.1618	1
Electric drives (Scroll expander)	W (kW)	10–100	3.3635 1.4191 −0.1798	3.5
Thermal oil heater	W (kW)	1–10,000	1.1979 1.4782 0.0958	2
Water heater	W (kW)	1–10,000	2.0829 0.9074 −0.0243	2

The costs predicted by the MCT were validated against real data for the size ranges listed in Table 3. The cost of investment of double-stage radial turboexpanders were evaluated considering each stage as a single component. The maximum size of scroll expander was 100 kW, in accordance with the

commercial availability of this kind of machine. Thus, when the size passes that limit, the installation in batteries of multiple units is considered. Expander sizes that are lower than 10 kW cannot be evaluated with the MCT. Therefore, the following cost functions were used when the expanders' size ranged between 1 and 10 kW.

$$\text{Radial turboexpander-generator} \qquad C_{RE} = 5647.89 \cdot P^{0.673} \tag{17}$$

$$\text{Scroll expander-generator} \qquad C_{SE} = 706.0 \cdot P^{0.673} \tag{18}$$

where C (€) is the total investment cost and P (kW) is the power size of the equipment. These equations were obtained by interpolating data provided by manufacturers. The annual maintenance costs were set equal to 2% and 1% of the investment cost for the expander-generators and gas-fired heaters, respectively. The MCT does not provide specific cost functions for the CHP-ICE and heat pumps. Therefore, several manufacturers' data were interpolated to generate the following cost functions:

$$\text{CHP-ICE} \qquad C_{ICE} = 5647.89 \cdot {Q_{ph}}^{0.7074} \tag{19}$$

$$\text{Maintenance (CHP-ICE)} \qquad M_{\%} = 0.1932 \cdot e^{-0.001 \cdot Q_{ph}} \cdot 100 \tag{20}$$

$$\text{Geothermal-HP} \qquad C_{GHP} = -0.2823 \cdot \ln\left(Q_{ph}\right) + 3.618 \tag{21}$$

$$\text{Air-HP} \qquad C_{AHP} = -0.1877 \cdot \ln\left(Q_{ph}\right) + 2.253 \tag{22}$$

where M (%) is the annual maintenance cost of ICEs given as percentage of the total investment cost. The annual maintenance cost of the heat pumps was set equal to 1.5% of the total investment cost. The required lifetime of the energy recovery systems was 25 years. The CHP-ICEs can run up to 90,000 h, corresponding to about 10 years of continuous operation. As a result, this preheating system is substituted every 10 years and the corresponding investment costs are to be considered.

3.5.2. Cost of Operation, Taxes, and Electricity Value

The cost of operation is related to the consumption of natural gas in the expander preheating systems (it is equal to zero in the case of heat pumps). The natural gas consumption depends on the performance of the preheating systems, as described in Section 3.3.2. Note that when the energy recovery system is not sized for the maximum capacity of the station ($\dot{m}_{DP} < \dot{m}_{step=1}$), a fraction of the natural gas flow rate is expanded and preheated (if required) using the traditional throttling valve system coupled to gas-fired heaters. The average cost of natural gas was set to 0.15 €/Stm3. Table 4 summarizes the costs associated with the production of electricity imposed by the Italian legislation [33]. Note that these costs are valid even if the electricity is totally self-consumed (heat pumps).

Table 4. Cost associated with the electricity production (taxes).

Primary Production Ranges (kWh/month)	Secondary Production Ranges (kWh/month)	Costs
E_{el} < 1,200,000.00	E_{el} < 200,000.00	0.0125 (€/kWh)
	200.00,00 < E_{el} < 1,200,000.00	0.0075 (€/kWh)
E_{el} > 120,000.00	E_{el} < 200,000.00	00125 (€/kWh)
	E_{el} > 20,000.00	4820 (€)

The value of the electric energy sold to the grid (I (€/kWh)) is obtained by Equation (23), which derives from interpolation of historical data. Its decreasing trend was caused by the increasing penetration of renewables in the electricity market.

$$I = 0.000179 \cdot (year + 2019) - 0.311 \tag{23}$$

where year is an integer number, used when the investment was made after 2019, representing the number of years after 2019.

3.5.3. Selection of the Dominating Solutions

The solutions provided by the economic analysis are considered feasible only when the PBP is lower than the lifetime of the systems (25 years) and when the NPV is a positive value. For each PRS class, the most convenient solutions were selected using a "dominating" criterion because of the two possible objectives (maximization of NPV or minimization of PBP). For instance, Figure 11 shows the economically feasible solutions resulting from the economic analysis conducted on the PRS class No. 3. The solutions that dominated the others are those linked by blue dots, which in this case corresponded to scroll expander-generators coupled to gas-fired heaters of different sizes.

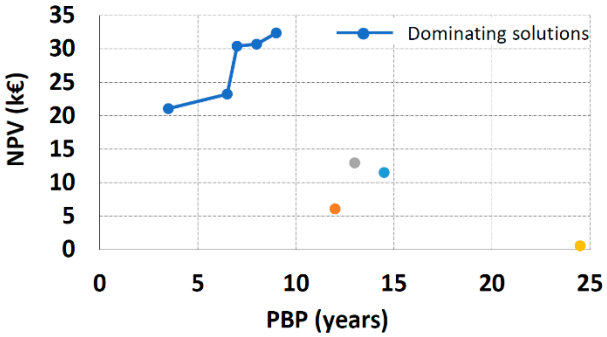

Figure 11. Example of the most economically feasible solutions (linked dots) selected using the "dominating" criterion among the possible ones. (The possible solutions provided in the example are related to PRS class No. 3).

4. Results

Table 5 shows the dominating solutions for each PRS class. In case of multiple dominating solutions, Table 5 shows the range of variability of NPV, PBP, and ε (see Equation (12)).

Table 5. Dominating energy recovery solutions for each PRS class.

PRS Classes	Energy Recovery Solution	PBP (Year)	NPV (€)	ε
1	Scroll	7–10	600–1400	0.03–0.09
2	Scroll_H	4–12	10,800–14,000	0.15–0.30
3	Scroll_H	3.5–9	21,000–32,500	0.08–0.20
4	Scroll_H	3	154,000	0.20
5	Scroll_H	14	1500	0.26
6	Scroll_H	4	17,000	0.26
7	Scroll_H	8	30,000	0.27
8	i.Scroll_H Scroll_ICE	i.7.5 7–9	i.110,761 58,000–175,000	i.0.23 0.22–0.33
9	-	-	-	-
10	-	-	-	-
11	-	-	-	-
12	Scroll_ICE	9.5	4080	<0

The results in Table 5 indicate that the most convenient solutions were always the scroll expanders coupled to gas-fired heaters or ICEs. The ICEs became competitive only at high-power classes having

medium-to-high expansion ratios (classes Nos. 8 and 12). Classes Nos. 9, 10, and 11 did not show feasible solutions due to the high temperature of preheating (i.e., high expansion ratio), which implied high costs that cannot be repaid in a reasonable period because of the low power generated. Class No. 1 did not indicate any need of preheating because of the low expansion ratio and the corresponding low isentropic efficiency of scroll expanders. For a given energy recovery technology, the PBP and NPV increased with the size of the system (i.e., on $\dot{m}_{DP}$). The ranges of PBP and NPV shown in classes Nos. 1, 2, and 3 (corresponding to low expansion ratio and small available power) suggest that maximizing NPV is never worth the related increase of the PBP. Thus, small size heat recovery systems should be considered as the most proper solutions for these classes. Conversely, in classes having high available power and medium-to-high expansion ratios the choice of the energy recovery system size depends upon the investor objective. For example, in class No. 8, increasing the size of Scroll_ICE systems from the minimum to the maximum value might be an option, because it triples the NPV with an increase of the PBP of only two years. Considering that a reasonable PBP should be lower than four years, only the PRSs included in classes Nos. 2, 3, 4, and 6 are feasible for a commercial diffusion of the proposed energy recovery systems. Results show also that the energy recovery efficiency (Equation (12)) of the proposed solutions ranged from 3 to 30%, depending on the size of the systems. Clearly, the increase of the size corresponds to an increase of the energy recovery efficiency because more of the available energy can be recovered by the system. Table 6 shows the total amount of the available and recoverable energy from all the 9000 PRSs that were included in the sample.

Table 6. Recoverable energy at PRS classes.

PRS Classes	Available Energy (GWh/Year)	Recoverable Energy (GWh/Year)	Recoverable Energy (%)
1	8.6	0.26–0.77	3–9
2	25.7	3.85–7.71	15–30
3	11.5	0.92–2.30	8–20
4	14.5	2.9	20
5	72.4	18.8	26
6	27.5	7.1	26
7	14.8	4.0	27
8	65.0	14.9–21.4	23–33
9	46.9	0	0
10	14.4	0	0
11	46.9	0	0
12	35.8	0	0

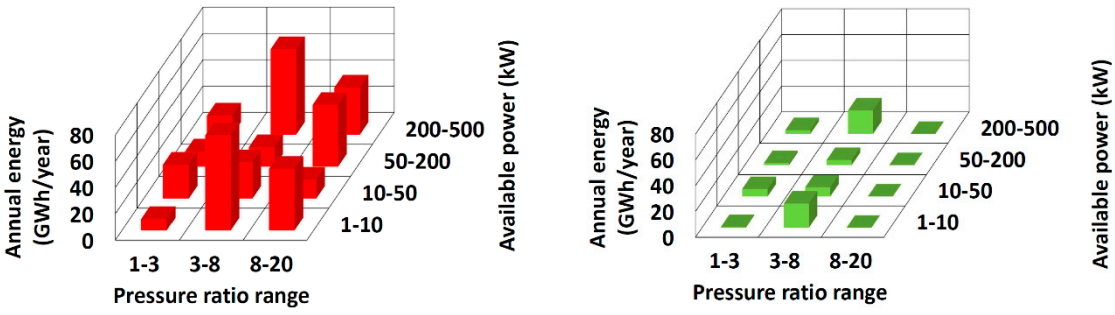

Figure 12. (**a**) Annual available energy and (**b**) annual recoverable energy from the 9000 pressure reduction stations, part of the sample and allocated to the corresponding classes (pressure ratio and available power).

It appears that the percentage of the recoverable energy from the dominating economically feasible solutions ranges between 13.7% and 16.9%. Note that class No. 12 did not contribute to the recoverable energy calculations even if Table 5 showed an economically feasible solution for this PRS class. This is due to the large consumption of natural gas of ICEs that involves a primary energy consumption that

is higher than the recovered energy from the pressure drop of natural gas. Figure 12 allows for a graphic representation of the results shown in Table 6. In particular, it allocates in the various PRS classes the overall annual available and recoverable energy from the 9000 PRSs included in the sample. Figure 12 highlights that the highest amount of energy is recoverable from PRSs featuring medium pressure ratios.

5. Conclusions

This paper clarifies the reasons behind the poor diffusion of energy recovery systems installed in the gas distribution networks, and provides useful guidelines about the features of the pressure reduction stations (PRSs) that make the installation of specific energy recovery technologies convenient. The example of application refers to the Italian gas distribution networks but has general characteristics that makes it applicable to other similar networks.

The main outcomes of the work are:

- The natural gas flow rate through the majority of PRSs is relatively low (<2000 Stm3/h), and so is the contribution to the energy recovery: The annual-averaged available power of 95% of the PRSs is lower than 50 kW. Currently, the few existing recovery systems are based on turboexpander-generators installed in PRSs with very large natural gas flow rates, indicating their convenience only for high-power stations.
- The economic analysis confirmed that radial turboexpander-generators are not economically feasible in PRSs having an available power between 1 and 500 kW and expansion ratios between 1 and 20.
- Scroll expanders are the most economically doable solution when coupled with gas-fired heaters in the whole range of available power and low-to-medium expansion ratios. They are convenient also when coupled with internal combustion engines in PRSs with high available power and medium-to-high expansion ratios. These volumetric and low-cost expanders seem to open the way for a wide application of energy recovery systems in PRSs.
- Only when the expansion ratios of the PRSs are lower than 3 and the available power is between 10 and 500 kW, can the energy recovery systems be paid off within reasonable periods (<4 years).
- The three classes of PRSs with high expansion ratios (>8) and low-to-medium available power (up to 200 kW) are neither thermodynamically nor economically suitable for energy recovery because of the high costs of the heating devices supplying the high-temperature thermal energy for preheating. Only if the available power is higher than 200 kW is the energy recovery system, including a cogeneration internal combustion engine (CHP-ICE), economically viable in spite of the consumption of fuel that is higher than the energy recovered. Thus, this PRSs with high expansion ratios cannot be considered for energy recovery.
- Using the economically feasible solutions, the total recoverable energy from the 9000 PRSs belonging to the Italian gas distribution network is approximately 15% (60 GWh/year) of the total available energy from the same PRSs (384 GWh/year).

The above findings allow assessing that small-size and low-cost energy recovery systems should be employed to achieve a large-scale diffusion of these systems. The costs and performance of other types of volumetric expanders should be further investigated to find the most convenient one for these applications.

Author Contributions: Writing—original draft preparation, P.D.; co-writer, G.C.; supervision, A.L. All authors have read and agreed to the published version of the manuscript.

Funding: This research received no external funding.

Acknowledgments: The authors acknowledge Pietro Fiorentini S.p.A. and Veil Energy for the support and the data supply.

Conflicts of Interest: The authors declare no conflict of interest.

Nomenclature

Acronyms	
PRS	Pressure reduction station
PBP	Payback period
NPV	Net present value
LNG	Liquified natural gas
HE	Heat exchanger
O&M	Operation and maintenance
GHP	Geothermal heat pump
AHP	Air heat pump
COP	Coefficient of performance
HP	Heat pump
CHP	Combined heat and power
ICE	Internal combustion engine
MCT	Module costing technique
CEPCI	Chemical engineering plant cost index
Symbols	
$\dot{m}$	Mass flow rate, kg/s
T	Temperature, °C
h	Enthalpy, kJ/(kg K)
P	Power, kW
p	Pressure, bar
A	Size parameter, kW
H	Gas-fired heater
E	Energy, GWh/year
Q	Heat flux, kW
M	Maintenance cost, €
I	Electric energy value, €/kWh
U	Blade tip speed, m/s
C_0	Isentropic spouting velocity, kJ/kgK
K_1, K_2, K_3	MCT factors dependent upon equipment type
C_P^0	MCT base conditions' equipment cost
C_{BM}	MCT bare module equipment cost
F_{BM}	MCT bare module factor
Y	MCT actualization factor
C	Cost, €
F_0	Cost of investment
k	Actualization factor
$F_{(year)}$	Actualized revenue
Greek symbols	
η	Efficiency
ε	Heat recovery system efficiency
Δt	Time step, s
Δh	Enthalpy difference, kJ/kgK
Subscripts and superscripts	
DP	Design point
av	Available
net	Net energy or power output
out	Outlet
in	Inlet
avg	Average
step	Time step
RE	Radial expander
SE	Scroll expander
evap	Evaporation
exp	Expander
is	Isentropic
th	Thermal
ph	Preheating
fuel	Preheating system fuel
cond	Condensation
ref	Reference efficiency
el	Electric

References

1. White, G.W. The Design of Gas Pipelines. *Pipeline Gas J.* **2012**, *9*, 239.
2. Bloch, H.P.; Soares, C. *Turboexpanders and Process Applications*; Gulf Professional Publishing: Houston, TX, USA, 2001.
3. Rheuban, J. Turbo Expanders: Harnessing the Hidden Potential of Our Natural Gas Distribution System. Available online: https://jacobrheuban.com/2009/03/09/turboexpanders-harnessing-the-hidden-potential-of-our-natural-gas-distribution-system/ (accessed on 19 April 2020).
4. Mirandola, A.; Minca, L. Energy Recovery by Expansion of High Pressure Natural Gas. In Proceedings of the 21st Intersociety Energy Conversion Engineering Conference, San Diego, CA, USA, 25–29 August 1986; pp. 16–21.
5. Mirandola, A.; Macor, A. Experimental Analysis of an Energy Recovery Plant by Expansion of Natural Gas. In Proceedings of the 23rd Intersociety Energy Conversion Engineering Conference, Denver, CO, USA, 31 July–5 August 1988; pp. 33–38.
6. Diao, A.; Wanga, Y.; Guo, Y.; Feng, M. Development and Application of Screw Expander in Natural Gas Pressure Energy Recovery at City Gas Station. *Appl. Therm. Eng.* **2018**, *142*, 665–673. [CrossRef]
7. Howard, C.; Oosthuizen, P.; Peppley, B. An Investigation of the Performance of a Hybrid Turboexpander-Fuel Cell System for Power Recovery at Natural Gas Pressure Reduction Stations. *Appl. Therm. Eng.* **2011**, *31*, 2165–2170. [CrossRef]

8. Yao, S.; Zhang, Y.; Deng, N.; Yub, X.; Dong, S. Performance Research on a Power Generation System Using Twin-Screw Expanders for Energy Recovery at Natural Gas Pressure Reduction Stations under Off-Design Conditions. *Appl. Energy* **2019**, *236*, 1218–1230. [CrossRef]
9. Yaxuan, X.; Shuoa, A.; Penga, X.; Yulong, D.; Chuan, L.; Qunli, Z.; Hongbing, C. A Novel Expander-Depending Natural Gas Pressure Regulation Configuration: Performance Analysis. *Appl. Energy* **2018**, *220*, 21–35.
10. Tian, Y.; Xing, Z.; He, Z.; Wu, H. Modeling and Performance Analysis of Twin-Screw Steam Expander under Fluctuating Operating Conditions in Steam Pipeline Pressure Energy Recovery Applications. *Energy* **2017**, *141*, 692–701. [CrossRef]
11. Barbarelli, S.; Florio, G.; Scornaienchi, N.M. Theoretical and Experimental Analysis of a New Compressible Flow Small Power Turbine Prototype. *Int. J. Heat Technol.* **2017**, *35*, S391–S398. [CrossRef]
12. Kolasiński, P.; Pomorski, M.; Błasiak, P.; Rak, J. Use of Rolling Piston Expanders for Energy Regeneration in Natural Gas Pressure Reduction Stations—Selected Thermodynamic Issues. *Appl. Sci.* **2017**, *7*, 535. [CrossRef]
13. Farzaneh-Gord, M.; Izadi, S.; Deymi-Dashtebayaz, M.; Pishbin, S.I. Optimizing Natural Gas Reciprocating Expansion Engines for Town Border Pressure Reduction Stations Based on AGA8 Equation of State. *J. Nat. Gas Sci. Eng.* **2015**, *26*, 6–17. [CrossRef]
14. Jannatabadi, M.; Farzaneh-Gord, M.; Rahbari, H.R.; Nersi, A. Energy and Exergy Analysis of Reciprocating Natural Gas Expansion Engine Based on Valve Configurations. *Energy* **2018**, *158*, 986–1000. [CrossRef]
15. Farzaneh-Gord, M.; Arabkoohsar, A.; Deymi Dasht-bayaz, M.; Machado, L.; Koury, R.N.N. Energy and Exergy Analysis of Natural Gas Pressure Reduction Points Equipped with Solar Heat and Controllable Heaters. *Renew. Energy* **2014**, *72*, 258–270. [CrossRef]
16. Borelli, D.; Devia, F.; Lo Cascio, E.; Schenone, C. Energy Recovery from Natural Gas Pressure Reduction Stations: Integration with Low Temperature Heat Sources. *Energy Convers. Manag.* **2018**, *159*, 274–283. [CrossRef]
17. Lo Cascio, E.; Borelli, D.; Devia, F.; Schenone, C. Future Distributed Generation: An Operational Multi-Objective Optimization Model for Integrated Small Scale Urban Electrical, Thermal and Gas Grids. *Energy Convers. Manag.* **2017**, *143*, 348–359. [CrossRef]
18. Farzaneh-Gord, M.; Ghezelbash, R.; Said, M.; Moghadam, A.J. Integration of Vertical Ground-Coupled Heat Pump into a Conventional Natural Gas Pressure Drop Station: Energy, Economic and CO_2 Emission Assessment. *Energy* **2016**, *112*, 998–1014. [CrossRef]
19. Ghanaee, R.; Foroud, A.A. Enhanced Structure and Optimal Capacity Sizing Method for Turbo-Expander Based Microgrid with Simultaneous Recovery of Cooling and Electrical Energy. *Energy* **2019**, *170*, 284–304. [CrossRef]
20. Yao, S.; Zhang, Y.; Yu, X. Thermo-Economic Analysis of a Novel Power Generation System Integrating a Natural Gas Expansion Plant with a Geothermal ORC in Tianjin, China. *Energy* **2018**, *164*, 602–614. [CrossRef]
21. Mirandola, A.; Macor, A.; Lazzaretto, A. Comparison between Energetic and Economic Optimization of Energy Recovery Plants with Gas Expanders and Cogeneration Engines. *Int. J. Energy Environ. Econ.* **1992**, *2*, 47–55.
22. Khanmohammadi, S.; Ahmadi, P.; Atashkari, K.; Kamali, R.K. Design and Optimization of an Integrated System to Recover Energy from a Gas Pressure Reduction Station. *Prog. Clean Energy* **2015**, *1*, 89–107.
23. Maddaloni, J.D.; Rowe, A.M. Natural Gas Exergy Recovery Powering Distributed Hydrogen Production. *Int. J. Hydrogen Energy* **2007**, *32*, 557–566. [CrossRef]
24. SNAM S.p.A, Piano Decennale di Sviluppo delle reti di Trasporto di Gas Naturale 2016–2025. Available online: https://www.snam.it/ (accessed on 15 January 2020).
25. Whitfield, A.; Baines, N.C. *Design of Radial Turbomachines*; Longman Scientific & Technical: New York, NY, USA, 1990.
26. Zhang, X.J. Study on the Performance and Optimization of a Scroll Expander Driven by Compressed Air. *Appl. Energy* **2017**, *186*, 347–358. [CrossRef]
27. Barone, G.; Buonomano, A.; Calise, F.; Palombo, A. Natural Gas Turbo-Expander Systems: A Dynamic Simulation Model for Energy and Economic Analyses. *Therm. Sci.* **2018**, *22*, 2215–2233. [CrossRef]
28. IEA Heat Pump Centre (HTP). Available online: https://www.heatpumpingtechnologies.org/ (accessed on 21 January 2020).

29. Sarbu, I.; Sebarchievici, C. Using Ground-Source Heat Pump Systems for Heating/Cooling of Buildings, Advances in Geothermal Energy. In *Advances in Geothermal Energy*; Ismail, B., Ed.; InTech: London, UK, 2015; Chapter 1; pp. 1–36.
30. Indoorcomfortmarketing. Available online: https://www.indoorcomfortmarketing.com/want-green-want-an-energy-efficient-system/ (accessed on 11 February 2020).
31. Veil-Energy. Available online: https://www.veil-energy.eu/ (accessed on 18 February 2020).
32. Turton, R.; Bailie, R.C.; Whiting, W.B.; Shaeiwitz, J.A. *Analysis, Synthesis and Design of Chemical Processes*, 3rd ed.; Turton, R., Ed.; Pearson: London, UK, 2009.
33. Testo Unico delle Accise. Available online: https://www.adm.gov.it/portale/-testo-unico-delle-accise (accessed on 14 May 2020).